Preliminary Monte Carlo based Inverse Model to Extract Optical Tissue Properties from Experimental Diffuse Reflectance Measurements

Coefficients Extraction for Gastrointestinal Dysplasia Detection

S. Pimenta[1], E. M. S. Castanheira[2] and G. Minas[1]
[1]*Centro Algoritmi, University of Minho, Campus de Azurém, Guimarães, Portugal*
[2]*Centre of Physics (CFUM), University of Minho, Campus de Gualtar, Braga, Portugal*

Keywords: Gastrointestinal Cancer, Spectroscopy, Diffuse Reflectance, Monte Carlo Simulations, Absorption Coefficient, Scattering Coefficient.

Abstract: The ability to detect cancer at its earliest stages, called "dysplasia", is the key of its successful treatment. Optical techniques, such as diffuse reflectance and intrinsic fluorescence, may improve the ability to detect gastrointestinal (GI) dysplasia since they have the potential to provide morphological and biochemical information of normal and malignant tissues. However, those optical tissue properties can only be provided if it is possible to extract information from the measured diffuse reflectance and intrinsic fluorescence signals. This paper presents the implementation and the validation of a preliminary Monte Carlo based inverse model to extract optical tissue properties, such as the absorption and the scattering coefficients, from diffuse reflectance experimental measurements in phantoms.

1 INTRODUCTION

The detection of cancer in its initial stage is one of the major goals of biomedical research. Gastrointestinal (GI) cancers are usually preceded by pre-cancerous changes and its early detection, especially at the dysplasia stage (before macroscopically visible changes occur on the tissues), will increase the chances of a successful treatment to the patient, improving the survival rate (Georgakoudi et al., 2001, Ell, 2003, Yu et al., 2008b).

A GI dysplasia is difficult to detect by visual inspection during endoscopy or colonoscopy, due to the lack of macroscopically easily visible changes on the tissues that occur during the early stage of cancer. Therefore, a large number of biopsies are performed in order to increase the detection probability of these invisible lesions (Georgakoudi et al., 2001, Ell, 2003, Mayinger et al., 2003). However, biopsies are procedures with sampling errors (since the sample condition could not be representative of the tissue malignant stage), high cost and are uncomfortable to the patients. Finally, their results are not immediately available, resulting on a delay of patient's treatment (Yu et al., 2008b, Georgakoudi, 2006).

For all these reasons, in recent years, there has been a strong interest towards the development of new methods for a more objective detection of the differences between premalignant and normal GI tissues. Epithelial tissues acquire altered optical properties during disease progression, especially due to the changes on their morphological and biochemical features. Spectroscopic techniques, especially diffuse reflectance and intrinsic fluorescence, have received special attention, due to their potential to detect small changes in the tissues. These techniques are based on light-tissues interactions, allowing the detection of macroscopically invisible lesions on the tissue surface, in other words, lesions at the dysplastic stage (Georgakoudi et al., 2001, Ell, 2003, Yu et al., 2008b, Georgakoudi, 2006).

Concerning diffuse reflectance measurements, it is used white light that is directed to the epithelial tissues where it is absorbed and scattered, and part of it returns to the tissue's surface with information about its optical properties. For the gastrointestinal tissues, absorption is mainly due to the presence of

Pimenta S., Castanheira E. and Minas G..
Preliminary Monte Carlo based Inverse Model to Extract Optical Tissue Properties from Experimental Diffuse Reflectance Measurements - Coefficients Extraction for Gastrointestinal Dysplasia Detection.
DOI: 10.5220/0004790201140121
In *Proceedings of 2nd International Conference on Photonics, Optics and Laser Technology* (PHOTOPTICS-2014), pages 114-121
ISBN: 978-989-758-008-6

hemoglobin, while scattering is caused by the collagen fibers present in the connective tissue. An increase in hemoglobin concentration, related to the angiogenesis (due to the early cancer progression), results in a reduction of the diffuse reflectance signal. Moreover, with cancer progression, the epithelial thickness increases, which reduce the quantity of light that reaches the collagen fibers. Thus, a decrease in scattering also causes a decrease of diffuse reflectance signal (Georgakoudi et al., 2001, Yu et al., 2008b, Georgakoudi, 2006).

Regarding intrinsic fluorescence (fluorescence without diffusion or absorption distortions), epithelial tissues produce fluorescence when excited by ultraviolet (UV) or blue-wavelength visible light. GI tissues have multiple fluorophores related to the cell structure and metabolism, such as collagen and NADH, which are known as markers of pre-cancerous changes. A decrease of collagen and an increase of NADH could be related to dysplasia progress, which results in a change of the fluorescence signal (Georgakoudi et al., 2001, Ell, 2003, Georgakoudi, 2006, Skala et al., 2004).

The intensity and shape of diffuse reflectance and intrinsic fluorescence spectra are dependent on the tissues pathological state and, therefore, its measurement can be used to extract information about the degree of tissue's malignancy. Several authors (Georgakoudi et al., 2001, Ell, 2003, Yu et al., 2008b) have developed prototypes that include those spectroscopy measurements for an accurate detection of GI dysplasia. However, their spectroscopy systems use expensive, complex and bulky illumination and detection equipments, e.g., xenon arc lamps or UV lasers, optical fibers, high quantum efficiency detectors and spectrographs that may hamper its integration in several endoscopic equipments.

Other groups have tried to develop spectroscopy microsystems (Yu et al., 2008a, Lo et al., 2009). Such microsystem, due to its small size, could be used at any screening room. Yu *et al.* developed a system to extract optical tissues properties from diffuse reflectance signal, based on the use of photodiodes as detectors. However, a monochromator, a xenon lamp and optical fibers were still used for illumination, which makes complex the system miniaturization. Lo *et al.* developed a system to measure tissues' diffuse reflectance signal, based on the use of LEDs (Light Emission Diodes), as a light source, and photodiodes, as light detectors. Despite this great advance in reducing cost and size, the authors only used five LEDs, which may not be enough to extract information for a complete diagnosis of dysplasia.

Thus, the development of a spectroscopy microsystem on a chip, without the need of regular optical fibers or spectrometer, that might be used *in-loco*, will have a high clinical value and represents the main innovation of the target project under this paper. The miniaturized system will be portable and may be integrated, for example, in endoscopes or colonoscopes, reducing the limitations of the existing methods for the early detection of GI dysplasia.

The microsystem is going to combine the implementation of two optical techniques – diffuse reflectance and intrinsic fluorescence – and the concept of thin-film optical filters deposited on silicon photodiodes. Miniaturized LEDs will be incorporated on the chip, featuring illumination sources for fluorescence and diffuse reflectance measurements. The model presented in this paper will extract information of the optical tissue properties from the diffuse reflectance measurements.

2 METHODOLOGY

As previously described in detail (Pimenta et al., 2013), to achieve the objectives described above, towards the microsystem implementation, the work is divided in several phases. Then, the main tasks of the project are presented:

- Spectrophotometric measurements in order to determine the relevant wavelengths/spectral bands for the detection of GI dysplasia and determine if the spectroscopic signals are temperature dependent;
- Implementation of mathematical models to extract optical tissue properties from diffuse reflectance and fluorescence measured signals;
- Design and fabrication of optical filters based on Fabry-Perot thin-film optical resonators and centered in the relevant wavelengths;
- Design and fabrication of photodiodes with improved quantum efficiency at the relevant spectral bands.
- Selection of miniaturized ultraviolet and white-light LEDs for fluorescence and diffuse reflectance measurements, respectively;
- Microsystem implementation and test.

3 WORK DEVELOPED

This section presents the experimental work that has already been developed by the research team, towards the spectroscopy microsystem implementation.

3.1 Validation of the Relevant Spectral Bands for Diagnosis

Studies performed by D. S. Ferreira (Ferreira et al., 2011b, Ferreira et al., 2011a) concluded that 16 spectral bands (between 350 nm and 750 nm) would be an appropriate number of wavelengths for diagnosis of dysplasia. The authors designed 16 thin-films optical filters centered in 16 spectral bands, and six of them were fabricated, at INESC-MN, Lisbon. The validation of the fabricated optical filters to extract spectroscopic signals was performed with commercial equipment and phantoms. As future work, the thin-film optical filters centered in wavelengths in near-UV/blue and near infra-red wavelength range will be improved.

3.2 Temperature Dependence of the Diffuse Reflectance Signal

In order to evaluate the temperature dependence of the diffuse reflectance signal, experimental measurements with a set of phantoms were performed, at four different temperatures: Tr (room temperature), T1 (37 ºC), T2 (40 ºC) and T3 (42 ºC).

Thus, a set of liquid homogeneous phantoms were created, with variable concentrations of an absorber (hemoglobin) and a scatterer (intralipid), in order to simulate tissues with variable properties. The hemoglobin (Hb) used is water soluble and was obtained from *Sigma-Aldrich* (H0267). The intralipid used is a 20% emulsion and was also obtained from *Sigma-Aldrich* (I141). During the experimental tests, it was assumed that the hemoglobin oxygenation was constant.

Table 1 shows the combinations of phantoms created to the temperature tests. The experimental measurements were performed in a commercial UV-Vis-IR spectrophotometer (*Shimadzu UV-3101PC*) equipped with integrating sphere.

Figure 1 shows the results for the phantom 5. As it can be seen, the diffuse reflectance signal is similar for all the temperatures tested. Similar results were obtained for all the phantoms, which allow concluding that the temperature of the sample does not affect the diffuse reflectance signal. Thus, to extract the optical properties of a tissue, from the diffuse reflectance signal, it is not necessary to consider its temperature.

Table 1: Created phantoms for temperature tests.

Phantom	Intralipid mass concentration	Hb concentration (mg/mL)
1	0.50	0.25
2	0.50	0.50
3	0.50	1.00
4	1.00	0.25
5	1.00	0.50
6	1.00	1.00
7	2.00	0.25
8	2.00	0.50
9	2.00	1.00

In the future, similar tests will be performed for the fluorescence signal.

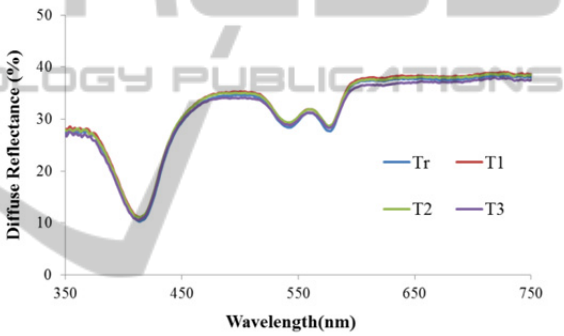

Figure 1: Diffuse reflectance spectra at different temperatures for phantom 5.

3.3 Implementation of a Model to Extract Tissue Properties

As previously mentioned, the intensity and shape of diffuse reflectance and fluorescence spectra are dependent on the tissues properties and its measurement can be used to extract information about the degree of tissues dysplasia. The extraction of these parameters requires the application of mathematical models.

3.3.1 Theoretical Considerations

The diffuse reflectance signal is affected by the absorption and scattering properties of the tissue, which are defined by absorption and scattering coefficients (μ_a and μ_s, respectively). μ_a is related with the concentration of chromophores in the tissue, for example hemoglobin, while μ_s is related with the size and concentration of scattering

molecules, such as collagen fibers in the epithelial tissues. Another important concept is the reduced scattering coefficient, μ_s', which is the μ_s with a corrected factor g (anisotropic factor) – equation (1). g is a factor that takes in account the angular dependence of a scattering event (it can vary from -1 [scattering in the backward direction] to 1 [scattering in the forward direction]), and its typical values for epithelial tissues are in the range of 0.7 to 0.95, across the wavelengths (λ) 750 nm to 350 nm, respectively (Yu *et al.*, 2008b, Georgakoudi, 2006, Zhu, 2007).

$$\mu_s'(\lambda) = \mu_s(\lambda)(1 - g(\lambda)) \quad (1)$$

The information carried on the diffuse reflectance signal is difficult to interpret due to the presence of combined absorption and scattering events. So, a change in the diffuse reflectance signal could be related with a change in absorption and/or scattering. Quantifying the affectation of each event on the diffuse reflectance signal, allows the possibility to extract μ_a and μ_s that define tissue optical properties.

Several authors have developed models to extract the absorption and scattering coefficients of tissues from diffuse reflectance experimental measurements. Some models are based on an approximation of the transport diffuse equation, developed by Zonios *et al*. in 1999 (Zonios et al., 1999). Despite the low computational intensity, these models are not suitable for a wide wavelength range of the electromagnetic spectrum.

Other models are based in Monte Carlo simulations (Bender et al., 2009, Palmer and Ramanujam, 2006, Yu et al., 2008a) and in a scaling approach developed by Graaff *et al.* (Graaff et al., 1993). Monte Carlo simulations allow the simulation of light propagation through a medium, such as a tissue, and based on the optical properties of the medium (μ_a and μ_s) obtaining the diffuse reflectance spectrum. The main advantages of these simulations are related to the facts that are suitable for a wide range of absorption and scattering coefficients and for a wide wavelength range of the electromagnetic spectrum (UV-Vis to NIR). Moreover, the accuracy of the model is dependent of the high contrast of the chromophore extinction coefficient, over the wavelengths, which happens with hemoglobin (Palmer and Ramanujam, 2006).

In this paper, it is presented a preliminary inverse model and its primary validation with liquid homogeneous phantoms, that allow extracting μ_a and μ_s from the diffuse reflectance signal, using a Monte Carlo forward model (freely available software (Wang and Jacques, 1995) and an equation that relates the diffuse reflectance with absorption and scattering coefficients of a tissue, presented in (Graaff et al., 1993). Equation (2) relates the diffuse reflectance of a tissue (normalized by the diffuse reflectance of a reference phantom with predefined optical properties) at each wavelength – $R_m(\lambda)$ with its optical properties as a function of wavelength - $\mu_a(\lambda)$ and $\mu_s(\lambda)$:

$$R_m(\lambda) = \sum_{j=1}^{N} N_{reflect}(j)\left(\frac{c(\lambda)}{c_{sim}(\lambda)}\right)^j \quad (2)$$

where N represents the mean number of interactions between each photon (that exits the tissue surface) and the medium. $N_{reflect}(j)$ is the portion of reflected photons after j interactions with the medium. $c(\lambda)$ represents the ratio $\frac{\mu_s(\lambda)}{\mu_s(\lambda)+\mu_a(\lambda)}$, that define the optical properties of the tissue. Finally, $c_{sim}(\lambda)$ represents the ratio $\frac{\mu_{s,sim}(\lambda)}{\mu_{s,sim}(\lambda)+\mu_{a,sim}(\lambda)}$, that define the optical properties of the reference phantom. As mentioned above, its diffuse reflectance (obtained with Monte Carlo forward model) will be used for normalizing the experimental diffuse reflectance of the tissue.

Thus, as first step it is necessary to choose a reference phantom with known optical properties that will be used in the forward Monte Carlo model to obtain its diffuse reflectance. It was used a liquid phantom with the following properties (similar to the phantom in (Graaff et al., 1993) in order to use the tabulated values for N and $N_{reflect}(j)$):

- Hemoglobin (absorber) concentration equal to 0.25 mg/mL;
- Intralipid (scatterer) mass concentration equal to 2%, representing collagen fibers.

Based on the knowledge of hemoglobin and intralipid concentration, it is possible to obtain the absorption and scattering coefficients that define the reference phantom as a function of wavelength ($\mu_{a,sim}(\lambda)$ and $\mu_{s,sim}(\lambda)$, respectively).

The absorption coefficient as a function of wavelength ($\mu_a(\lambda)$) could be obtained by the application of the equation (3):

$$\mu_a(\lambda) = \ln(10) \times \varepsilon_i(\lambda) \times C_i \quad (3)$$

where $\varepsilon_i(\lambda)$ is the extinction coefficient of the absorber, that defines its capacity to absorb light as a function of wavelength; C_i is the absorber concentration in the phantom.

The scattering coefficient as a function of wavelength could be obtained using the Mie theory for spherical particles, available as free software in

(Mätzler, 2002). The source code can be used in Matlab, given the volume fraction (vf = 0.1, for the reference phantom), refractive index (n = 1.362 (Ding et al., 2005)) and size (s = 456 nm (Choukeife and L'Huillier, 1999)) of the intralipid spheres and the refractive index of the surrounding medium, water in this case (n = 1.33).

Once the $\mu_{a,sim}(\lambda)$ and $\mu_{s,sim}(\lambda)$ are known, they could be used in the Monte Carlo forward model in order to obtain the diffuse reflectance of the reference phantom. As mentioned previously, it was used a free available software (precompiled PC version) (Wang and Jacques, 1995). However, some Matlab functions were created in order to introduce the features of the reference phantom in the model, according to the software manual available in (Wang and Jacques, 1995). The parameters used in the Monte Carlo simulation were: total number of photons (30000), $\mu_{asim}(\lambda)$, $\mu_{ssim}(\lambda)$, isotropic scattering (g=0), model dimensions (1cm(radius)× 1cm(depth)), phantom refractive index (1.332) and above/below refractive index medium (1.0 and 1.5, respectively).

As a second step, it is necessary to use a Matlab optimization function, *lsqcurvefit*, with initial random input solutions for absorption and scattering coefficients ($c(\lambda)$). This function is based on the least-squares algorithm and its main goal is iteratively updated $c(\lambda)$ until the value of modulated reflectance (equation (1) output) is similar to the experimental diffuse reflectance that define our phantom, allowing to extract its optical properties $\mu_a(\lambda)$ and $\mu_s(\lambda)$. It is important to note again that both diffuse reflectances (modulated and experimental) are normalized by the diffuse reflectance of the reference phantom (previously obtained with Monte Carlo forward model).

3.3.2 Tissue Phantoms

For a preliminary validation of the implemented model, a set of liquid homogeneous phantoms were created, with variable concentrations of the absorber, hemoglobin (0.27 mg/mL, 0.49 mg/mL and 1.03 mg/mL), and with a mass concentration of intralipid of 0.5%. The diffuse reflectance spectrum of each phantom was measured between 350 nm and 750 nm, using an UV-Vis-NIR spectrophotometer equipped with integrating sphere (*Shimadzu UV-3101PC*). Moreover, the wavelength-dependent hemoglobin extinction coefficient was obtained with the same spectrophotometer.

3.3.3 Validation of Monte Carlo Forward Model

Once the implemented inverse model uses the Monte Carlo forward model to obtain the diffuse reflectance of the reference phantom, it was performed a validation using the homogeneous phantoms created, for evaluating the accuracy of the free available software used (Wang and Jacques, 1995), in the achievement of the diffuse reflectance of a medium.

Thus, knowing the hemoglobin and intralipid concentrations, for each created phantom, the optical properties that define each of them – $\mu_a(\lambda)$ and $\mu_s(\lambda)$ – were obtained by the application of equation (3) and the freely available software for Mie theory. After that, these properties were used in a Monte Carlo simulation with the following parameters: total number of photons (30000), $\mu_a(\lambda)$, $\mu_s(\lambda)$, anisotropic scattering (g=0.8), model dimensions (1cm(radius) × 1cm(depth)), phantom refractive index (1.332) and above/below refractive index medium (1.0 and 1.5, respectively).

Figure 2 shows the ratio between the modeled diffuse reflectance (DR_{mod}) and the measured diffuse reflectance (DR_{exp}) for each created phantom as a function of wavelength. Despite the slight deviations from unity (the perfect agreement), especially in wavelengths that correspond to the hemoglobin absorption peaks (420 nm, 540 nm and 580 nm), in general it can be concluded that there is a good agreement between the modeled (obtained from Monte Carlo forward model) and the experimental/measured diffuse reflectance, since de ratio between them is close to unity across the analyzed wavelengths.

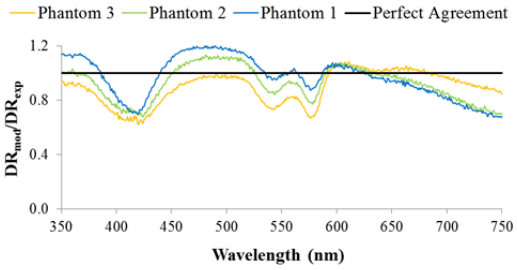

Figure 2: Ratio between the modeled diffuse reflectance (DR_{mod}) and the measured diffuse reflectance (DR_{exp}) spectra for each created phantom.

3.3.4 Validation of the Inverse Model

A preliminary validation of the implemented inverse model was performed using the created liquid phantoms. Thus, for each phantom, the optimization

function (*lsqcurvefit*) was repeated several times with different initial input solutions, for absorption and scattering coefficients, in order to increase the probability of extracting a global minimum. Moreover, the obtained coefficients were mathematically approximated, in order to ensure that the values follow the form of the equations that characterize them.

Next, the absorption and scattering coefficients extracted from the inverse model were compared with the expected/theoretical coefficients of each phantom. Figures 3 and 4 show the plots of the extracted *versus* expected absorption and reduced scattering coefficients, respectively, for all wavelengths and each created phantom.

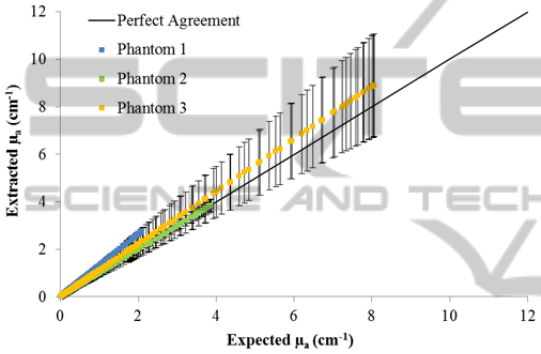

Figure 3: Extracted *versus* expected absorption coefficient ($\mu_a(cm^{-1})$) for each created phantom.

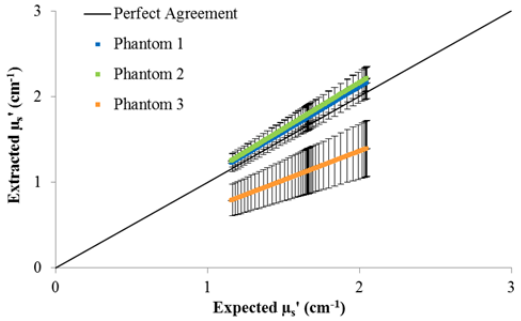

Figure 4: Extracted *versus* expected reduced scattering coefficient ($\mu_s'(cm^{-1})$) for each created phantom.

As it can be seen in figures 3 and 4, the implemented inverse model allows the extraction of the absorption and scattering coefficients with low differences between the expected and extracted tissue optical properties, especially for the absorption properties, since the extracted coefficients are very similar to the expected.

Concerning the reduced scattering coefficient, phantom 3 has a slight deviation from the expected result. So, in the future it will be important to evaluate if this deviation affects the final tissue diagnostic. If it is significant in the diagnostic result, the implemented model must be improved in order to avoid diagnostic errors.

3.3.5 Validation of the Inverse Model with the 16 Spectral Bands

As previously mentioned, studies performed by D. S. Ferreira (Ferreira *et al.*, 2011b, Ferreira *et al.*, 2011a) concluded that 16 spectral bands (350, 370, 380, 400, 420, 450, 480, 510, 540, 560, 580, 600, 620, 650, 700 and 750 nm) would be an appropriate number of wavelengths for diagnosis of dysplasia.

So, based on the diffuse reflectance values at the 16 spectral validated bands, it was reconstructed the total diffuse reflectance, for each phantom, using a Matlab fitting function – *spline*. The main advantage of using splines is related with the fact that they can be used to represent functions over large intervals, where it would be impractical to use a single approximating polynomial, since they are smooth piecewise polynomials.

Figure 5 shows the measured (experimental) diffuse reflectance spectra (blue curve – R1) and the reconstructed diffuse reflectance spectra (red curve – R1 recons) from phantom 1. As mentioned above, R1 recons are obtained based on the use of the 16 spectral bands previously validated (green points - Spectral bands) and the *spline* function.

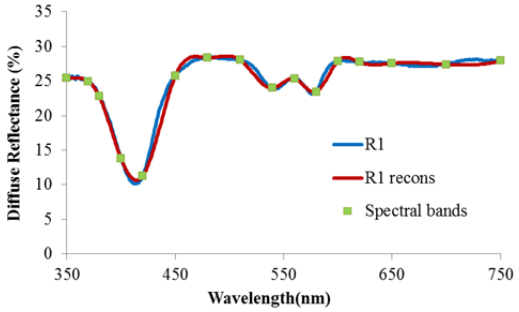

Figure 5: Diffuse Reflectance from phantom 1: experimental spectra (R1), reconstructed spectra (R1 recons) and the 16 spectral bands used for reconstruction (Spectral bands).

Based on the reconstructed spectra of the liquid created phantoms (1, 2 and 3), a validation of the implemented inverse model was performed, in order to compare the results obtained with the original or experimental spectra. Again, for each phantom, the optimization function (*lsqcurvefit*) was repeated several times with different initial input solutions, in order to extract the absorption and scattering

coefficients. Figures 6 and 7 show the plots of the extracted *versus* expected absorption and reduced scattering coefficients, respectively, for all wavelengths and for each created phantom.

As it can be seen in figures 6 and 7, the use of the reconstructed spectra (from the 16 spectral bands) in the implemented inverse model allows the extraction of the absorption and scattering coefficients with low differences between the expected and extracted tissue optical properties, especially for the absorption coefficient. As previously referred, some slight deviations in the reduced scattering coefficient must be evaluated.

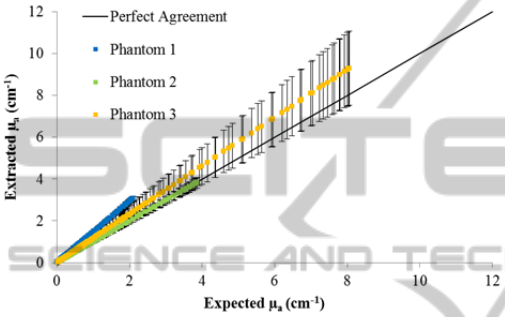

Figure 6: Extracted *versus* expected absorption coefficient ($\mu_a(cm^{-1})$), using the reconstructed spectra for each created phantom.

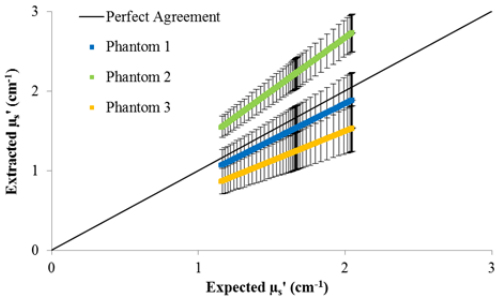

Figure 7: Extracted *versus* expected reduced scattering coefficient ($\mu_s'(cm^{-1})$), using the reconstructed spectra for each created phantom.

4 CONCLUSIONS AND FUTURE GUIDELINES

The work performed until now allow to conclude that the temperature of a tissue doesn't affect the diffuse reflectance signal. Similar tests will be performed for the fluorescence signal and using different phantoms.

The absorption and scattering properties of a tissue could be extracted from the diffuse reflectance signal, by the implementation of a Monte Carlo based inverse model. The extracted coefficients obtained, with a set of phantoms, were similar to the expected coefficients. Moreover, the implemented inverse model was validated using the reconstructed spectra of the phantoms, based only in 16 values of diffuse reflectance, for each phantom. This validation will allow the design and fabrication of optical filters and photodiodes, centered in these 16 spectral bands.

Nevertheless, in the future the model will be tested with more and different phantoms, for evaluating its accuracy in the extraction of optical tissue properties. Moreover, different reference phantoms will also be used to test their influence in the accuracy of the model.

Finally, the other tasks described in section 2 are ongoing towards the full microsystem implementation.

ACKNOWLEDGEMENTS

This work is funded by FEDER funds through the "Eixo I do Programa Operacional Fatores de Competitividade (POFC) QREN, project reference COMPETE: FCOMP-01-0124-FEDER-020241, and by FCT- Fundação para a Ciência e a Tecnologia, project reference PTDC/EBB-EBI/120334/2010. S. Pimenta thanks the FCT for the SFRH/BD/87605/2012 PhD grant.

REFERENCES

Bender, J. E., Vishwanath, K., Moore, L. K., Brown, J. Q., Chang, V., Palmer, G. M. & Ramanujam, N. 2009. A Robust Monte Carlo Model For The Extraction Of Biological Absorption And Scattering In Vivo. *IEEE Transactions On Biomedical Engineering,* 56**,** 960-968.

Choukeife, J. E. & L'huillier, J. P. 1999. Measurements Of Scattering Effects Within Tissue-Like Media At Two Wavelengths Of 632.8 Nm And 680 Nm. *Lasers In Medical Science,* 14**,** 286–296.

Ding, H., Lu, J. Q., Jacobs, K. M. & Hu, X.-H. 2005. Determination Of Refractive Indices Of Porcine Skin Tissues And Intralipid At Eight Wavelengths Between 325 And 1557 Nm. *Optical Society Of America,* 22**,** 1151-1157.

Ell, C. 2003. Improving Endoscopic Resolution And Sampling: Fluorescence Techniques. *Gut,* 52**,** 30-33.

Ferreira, D. S., Mirkovic, J., Wolffenbuttel, R. F., Correia, J. H., Feld, M. S. & Minas, G. 2011a. Narrow-Band Pass Filter Array For Integrated Opto-Electronic

Spectroscopy Detectors To Assess Esophageal Tissue. *Biomedical Optics Express,* 2**,** 1703-1716.

Ferreira, D. S., Pinto, V. C., H.Correia, J. & Minas, G. 2011b. Spectroscopic Detection Of Gastrointestinal Dysplasia Using Optical Microsensors. *Ieee Transactions On Biomedical Engineering,* 58**,** 2633-2639.

Georgakoudi, I. 2006. The Color Of Cancer. *Journal Of Luminescence,* 119-120**,** 75-83.

Georgakoudi, I., Jacobson, B. C., Dam, J. V., Backman, V., Wallace, M. B., Mueller, M. G., Zhang, Q., Badizadegan, K., Sun, D., Thomas, G. A., Perelman, L. T. & Feld, M. S. 2001. Fluorescence, Reflectance, And Light-Scattering Spectroscopy For Evaluating Dysplasia In Patients With Barrett's Esophagus. *Gastroenterology,* 120**,** 1620-1629.

Graaff, R., Koelink, M. H., Mul, F. F. M. D., Zijlstra, W. G., Dassel, A. C. M. & Aarnoudse, J. G. 1993. Condensed Monte Carlo Simulations For The Description Of Light Transport. *Applied Optics,* 32(4)**,** 426-434.

Lo, J. Y., Yu, B., Fu, H. L., Bender, J. E., Palmer, G. M., Kuech, T. F. & Ramanujam, N. 2009. A Strategy For Quantitative Spectral Imaging Of Tissue Absorption And Scattering Using Light Emitting Diodes And Photodiodes. *Optics Express,* 17**,** 1372-1384.

Mätzler, C. 2002. *Maetzler's Matlab Code For Mie Theory* [Online]. Available: Http://Omlc.Ogi.Edu/Software/Mie/ [Accessed Fevereiro 2013.

Mayinger, B., Jordan, M., Horner, P., Gerlach, C., Muehldorfer, S., Bittorf, B. R., Matzel, K. E., Hohenberger, W., Hahn, E. G. & Guenther, K. 2003. Endoscopic Light-Induced Autofluorescence Spectroscopy For The Diagnosis Of Colorectal Cancer And Adenoma. *Journal Of Photochemistry And Photobiology B: Biology,* 70**,** 13-20.

Palmer, G. M. & Ramanujam, N. 2006. Monte Carlo-Based Inverse Model For Calculating Tissue Optical Properties. Part I: Theory And Validation On Synthetic Phantoms. *Applied Optics,* 45(5)**,** 1062-1071.

Pimenta, S., Monteiro, T. S., Goncalves, L. M. & Minas, G. 2013. Spectroscopy And Ph Biosensors For The Detection Of Gastrointestinal Dysplasia. *Published In Proceedings Of Ieee Embs, 3rd Portuguese Bioengeneering Meeting, Braga, Portugal, 20-22 February*.

Skala, M. C., Palmer, G. M., Zhu, C., Liu, Q., Vrotsos, K. M., Marshek-Stone, C. L., Gendron-Fitzpatrick, A. & Ramanujam, N. 2004. An Investigation Of Fiber-Optic Probe Designs For Optical Spectroscopic Diagnosis Of Epithelial Pre-Cancers. *Lasers In Surgery And Medicine,* 34(1)**,** 25-38.

Wang, L. & Jacques, S. L. 1995. *(Mcml) Monte Carlo For Multi-Layered Media* [Online]. Available: Http://Omlc.Ogi.Edu/Software/Mc/ [Accessed Fevereiro 2013.

Yu, B., Lo, J. Y., Kuech, T. F., Palmer, G. M., Bender, J. E. & Ramanujam, N. 2008a. Cost-Effective Diffuse Reflectance Spectroscopy Device For Quantifying Tissue Absorption And Scattering In Vivo. *Journal Of Biomedical Optics,* 13**,** 060505.

Yu, C.-C., Lau, C., O'donoghue, G., Mirkovic, J., Mcgee, S., Galindo, L., Elackattu, A., Stier, E., Grillone, G., Badizadegan, K., Dasari, R. R. & Feld, M. S. 2008b. Quantitative Spectroscopic Imaging For Noninvasive Early Cancer Detection. *Optics Express,* 16**,** 16227-16239.

Zhu, C. 2007. *The Use Of Fluorescence And Diffuse Reflectance Spectroscopy For Breast Cancer Diagnosis.* Phd, University Of Wisconsin-Madison.

Zonios, G., Perelman, L. T., Backman, V., Manoharan, R., Fitzmaurice, M., Dam, J. V. & Feld, M. S. 1999. Diffuse Reflectance Spectroscopy Of Human Adenomatous Colon Polyps In Vivo. *Applied Optics,* 38**,** 6628-6637.